Comparison of the hydrodynamic and Dirac models of the dispersion interaction between graphene and H, He*, or Na atoms

Yu. V. Churkin, A. B. Fedortsov, G. L. Klimchitskaya, and V. A. Yurova

North-West Technical University, Millionnaya Street 5, St.Petersburg, 191065, Russia

Abstract

The van der Waals and Casimir-Polder interaction of different atoms with graphene is investigated using the Dirac model which assumes that the energy of quasiparticles is linear with respect to the momentum. The obtained results for the van der Waals coefficients of hydrogen atoms and molecules and atoms of metastable He* and Na as a function of separation are compared with respective results found using the hydrodynamic model of graphene. It is shown that, regardless of the value of the gap parameter, the Dirac model leads to much smaller values of the van der Waals coefficients than the hydrodynamic model. The experiment on quantum reflection of metastable He* and Na atoms on graphene is proposed which is capable to discriminate between the two models of the electronic structure of graphene. In this respect the parameters of the phenomenological potential for both these atoms interacting with graphene described by different models are determined.

PACS numbers: 73.22.Pr, 78.67.-n, 12.20.Ds

I. INTRODUCTION

It is common knowledge that dispersion force between two neutral atoms or molecules arises in second order perturbation theory from the dipole-dipole interaction [1]. This force takes its name from the fact that it is caused by the dispersions of dipole operators, i.e., by quantum fluctuations. At short separations, where the electromagnetic interaction can be considered as instantaneous, dispersion force depends only on one fundamental constant, the Planck constant $\hbar$. In this case it is referred to as the van der Waals force [2]. At larger separations, where the retardation of the electromagnetic interaction becomes significant, dispersion force depends on both $\hbar$ and the velocity of light c. In this case the force is usually called the Casimir-Polder force [3]. As a result of interatomic interactions, dispersion forces act also between an atom (molecule) and a macroscopic body and between two closely spaced macroscopic bodies (in the retarded regime, the force between two macrobodies is called the Casimir force [4]).

The van der Waals and Casimir-Polder forces between atoms (molecules) and material walls play an important role in different physical, chemical and biological phenomena [1, 2]. The magnitude and the distance dependence of these forces were measured in several experiments [5]. In the last few years atom-wall interaction is being studied intensively in connection with the phenomenon of quantum-reflection [6–13]. Theoretical description of atom-wall interaction is given by the Lifshitz theory [1, 2, 4, 5, 14] which expresses the van der Waals and Casimir-Polder energy and force through the dynamic electric polarizability of an atom and the frequency-dependent dielectric permittivity of wall material. A large body of research of atom-wall interactions for different atoms and wall materials on the basis of the Lifshitz theory has been performed in the literature [1, 2, 4, 5, 15–21].

Considerable recent attention was attracted to two-dimensional carbon nanostructures, such as graphene, carbon nanotubes and fullerenes [22]. Carbon nanostructures possess unique mechanical, electrical and optical properties which are of major fundamental and applied interest. One of potential applications of carbon nanostructures is to the problem of hydrogen storage [23]. Keeping in mind that one-atom-thick nanostructures are not characterized by the dielectric permittivity, the Lifshitz theory seems to be not immediately applicable. Because of this, dispersion interaction between hydrogen atoms (molecules) and a graphite sheet (graphene) or single-walled carbon nanotubes was investigated mainly by

using the phenomenological density functional theory [24–27]. The second-order perturbation theory was also used [28] to calculate line shifts of a two-level atom interacting with a nanotube. For the multiwalled carbon nanotubes with at least several walls, the concept of dielectric permittivity of graphite was shown to be applicable [29].

The application of the Lifshitz theory of dispersion interaction to one-atom-thick carbon nanostructures calls for introduction of some other quantity which determines the reflection coefficients instead of usually used dielectric permittivity. In order to extend the Lifshitz theory to the case of carbon systems, the description of graphene in terms of the two-dimensional free electron gas [30] was used. Graphene was considered as an infinitesimally thin positively charged flat sheet, carring a homogeneous fluid with some mass and negative charge densities (the hydrodynamic model). The interaction of the electromagnetic oscillations with such a sheet was described by the special reflection coefficients [31, 32]. The proposed approximate description was applied for the calculation of dispersion interaction between two parallel graphene sheets [33], between graphene and material plate [34], graphene and an atom or a molecule, and between an atom or a molecule and a single-walled carbon nanotube [35]. The hydrodynamic model, however, does not take into account that low-energy excitations in graphene are massless Dirac fermions except for the fact that they move with a Fermi velocity rather than with the speed of light [22, 36]. As a consequence, at low energies the dispersion relation for quasiparticles in graphene is approximately linear with respect to the momentum measured relatively to the corners of the graphene Brillouin zone. Under the assumption that these properties, which are referred to as the Dirac model, hold at any energy, the reflection coefficients for the electromagnetic oscillations on graphene were found [37]. These coefficients were used to calculate the Casimir interaction between a graphene and a parallel ideal metal plane [37].

In this paper we investigate the dispersion interaction of atoms (molecules) with graphene described by the Dirac model. We consider an atom and a molecule of hydrogen, and also atoms of metastable He^* and Na often used in experiments on quantum reflection. The van der Waals coefficient C_3 is computed by using the Lifshitz formula as a function of atom-graphene separation. The obtained results are compared with those obtained previously using the hydrodynamic model of the electronic structure of graphene. It is shown that in all cases the magnitudes of the van der Waals and Casimir-Polder energy computed with the help of the Dirac model are less than with the hydrodynamic model. Differences between the

two sets of results increase with the increase of separation. We also find the dependence of the predicted van der Waals and Casimir-Polder energies on the value of the gap parameter. We propose the experiment allowing to discriminate between the predictions of the Dirac and hydrodynamic models of graphene. For this purpose the parameters of phenomenological potential of atom-graphene interaction are determined for atoms of metastable He^* and Na.

The paper is organized as follows. In Sec. II we briefly present the Lifshitz formula for atom-wall interaction and the forms of reflection coefficients in both models. Section III contains computational results for the van der Waals coefficient C_3 as a function of separation and gap parameter for atoms and molecules of hydrogen. In Sec. IV similar results are presented for atoms of metastable He^* and Na. The parameters of phenomenological potential for these atoms are also determined for the needs of proposed experiment. In Sec. V the reader will find our conclusions and discussion.

II. TWO MODELS FOR INTERACTION OF ATOMS WITH GRAPHENE

The van der Waals and Casimir-Polder energy in the configuration of a microparticle (an atom or a molecule) and a plane structure can be expressed in terms of reflection coefficients of the electromagnetic oscillations on this structure in the following way [4, 14]

$$E(a)=-\frac{\hbar}{2\pi}\int_0^\infty d\xi\alpha(i\xi)\int_0^\infty k_\perp dk_\perp\, q\, e^{-2aq} \times\left\{2r_{\mathrm{TM}}(i\xi,k_\perp)-\frac{\xi^2}{q^2c^2}\left[r_{\mathrm{TM}}(i\xi,k_\perp)+r_{\mathrm{TE}}(i\xi,k_\perp)\right]\right\}. \tag{1}$$

Here, a is the separation distance between the microparticle and the plane, $k_\perp$ is the magnitude of the wave vector projection on the plane (the latter is perpendicular to the z axis), $\alpha(i\xi)$ is the dynamic polarizability of a microparticle calculated along the imaginary frequency axis, and $q^2=k_\perp^2+\xi^2/c^2$. The reflection coefficients for two independent polarizations of the electromagnetic field, transverse magnetic and transverse electric, $r_{\mathrm{TM,TE}}$, are also calculated along the imaginary frequency axis. In the framework of the scattering approach (see, for instance, Refs. [4, 38]) it can be proved that under some conditions Eq. (1) holds for any planar structure with appropriately chosen reflection coefficients. Specifically, the use of Eq. (1) is justified if a plane structure (a material of the plate or a graphene) is in thermal equilibrium with an environment at some not too high temperature, and an atom is in the ground state [15]. For instance, the probabilities that an atom is in an excited state

are distributed according to the Boltzmann law and are negligibly small at room temperature ($T = 300\,\mathrm{K}$). As a result, the zero-temperature Lifshitz formula (1) can be used at sufficiently small separations (see below for quantitative evaluation of its application region).

There are different models of reflection coefficients for graphene using different boundary conditions. In the framework of the hydrodynamic model of the electronic structure of graphene they can be presented in the form [31–35]

$$r_{\mathrm{TM}}(i\xi,k_\perp)\equiv r_{\mathrm{TM}}^{(h)}(i\xi,k_\perp)=\frac{c^2qK}{c^2qK+\xi^2},$$
$$r_{\mathrm{TE}}(i\xi,k_\perp)\equiv r_{\mathrm{TE}}^{(h)}(i\xi,k_\perp)=-\frac{K}{K+q}, \tag{2}$$

where the wave number of the graphene sheet $K = 6.75\times10^5\,\mathrm{m}^{-1}$ corresponds to the frequency $\omega_K = cK = 2.02\times10^{14}\,\mathrm{rad/s}$. As was explained in Sec. I, the hydrodynamic model does not take into account some important properties of graphene which hold at low energies, specifically that the energy of quasiparticles is a linear function of the momentum. These properties are well described by the Dirac model of the electronic structure of graphene where the reflection coefficients are given by [37]

$$r_{\mathrm{TM}}(i\xi,k_\perp)\equiv r_{\mathrm{TM}}^{(D)}(i\xi,k_\perp)=\frac{\alpha q\Phi(\tilde{q})}{2\tilde{q}^2+\alpha q\Phi(\tilde{q})},$$
$$r_{\mathrm{TE}}(i\xi,k_\perp)\equiv r_{\mathrm{TE}}^{(D)}(i\xi,k_\perp)=-\frac{\alpha\Phi(\tilde{q})}{2q+\alpha\Phi(\tilde{q})}. \tag{3}$$

Here $\alpha=e^2/(\hbar c)\approx1/137$ is the fine-structure constant, $\tilde{q}^2=(v_{\mathrm{F}}^2k_\perp^2+\xi^2)/c^2$, $v_{\mathrm{F}}\approx10^6\,\mathrm{m/s}$ is the Fermi velocity, and the function Φ determines the polarization tensor in an external electromagnetic field in the one-loop approximation in three dimensional space-time. The explicit form of this function along the imaginary frequency axis is the following [37]

$$\Phi(\tilde{q})=N\left(\tilde{\Delta}+\frac{\tilde{q}^2-4\tilde{\Delta}^2}{2\tilde{q}}\,\arctan\frac{\tilde{q}}{2\tilde{\Delta}}\right), \tag{4}$$

where for graphene $N=4$, $\tilde{\Delta}=\Delta/(\hbar c)$, and the value of the gap parameter Δ is not well known. The upper bound on Δ is approximately equal to $0.1\,\mathrm{eV}$, but it might be also much smaller [22, 37].

Below, we perform computations of the van der Waals and Casimir-Polder interaction energy between different atoms and graphene. For this purpose it is useful to introduce the dimensionless variable $y=2qa$ instead of $k_\perp$. Then Eq. (1) can be identically rewritten in

the form

$$E(a) = -\frac{C_3(a)}{a^3}, \tag{5}$$

where the van der Waals coefficient $C_3(a)$ is given by

$$C_3(a) = \frac{\hbar}{16\pi}\int_0^\infty dy e^{-y}\int_0^{cy/(2a)} d\xi\alpha(i\xi) \times\left\{2y^2 r_{\rm TM}(i\xi,y) - \frac{4a^2\xi^2}{c^2}\left[r_{\rm TM}(i\xi,y)+r_{\rm TE}(i\xi,y)\right]\right\}. \tag{6}$$

Either the hydrodynamic- or Dirac-model reflection coefficients (2) and (3), respectively, can be substituted here keeping in mind that in terms of new variable it holds

$$q = \frac{y}{2a}, \quad \tilde{q} = \left[\frac{v_{\rm F}^2}{c^2}\frac{y^2}{4a^2} + \left(1-\frac{v_{\rm F}^2}{c^2}\right)\frac{\xi^2}{c^2}\right]^{1/2}. \tag{7}$$

Notice that Eq. (5) with constant C_3 presents the energy of nonretarded van der Waals interaction between an atom and a wall which is valid only at small separations of about 2–3 nm[1, 2, 4, 5, 14–16] (at shorter separations the description of graphene by means of the boundary conditions becomes inapplicable and one should take into account an atomic structure of the sheet). If, however, C_3 depends on separation in accordance with Eq. (6), the interaction energy (5) includes both the nonretarded and retarded (relativistic) regimes. As a result, Eqs. (5) and (6) are applicable up to separation distances where the thermal effects become significant. It is well known [4, 15] that at room temperature the zero-temperature Lifshitz formula provides very exact computational results of atom-plate interaction up to separations of about $1\,\mu$m (see Sec. IV for a computational example). As to the function Φ determining the polarization tensor, relativistic thermal quantum field theory does not predict a noticeable change of this quantity at room temperature, as compared to the case of zero temperature (note that computation in Ref. [39] was, strictly speaking, performed in a nonretarded regime).

III. INTERACTION OF HYDROGEN ATOMS AND MOLECULES WITH GRAPHENE

Here, we compare the van der Waals coefficients for interaction of hydrogen atoms and molecules with graphene in the cases when computations are performed with the help of Dirac and hydrodynamic models. To perform computations using Eq. (6), one needs some

expressions for the atomic and molecular dynamic polarizabilities of hydrogen. As was shown in Refs. [16, 29], for the calculation of dispersion forces, the polarizabilities can be represented with sufficient precision in the framework of single-oscillator model

$$\alpha(i\xi)=\frac{\alpha(0)}{1+\frac{\xi^2}{\omega_0^2}}, \tag{8}$$

where $\alpha(0)$ is the static polarizability and ω_0 is the characteristic frequency. For a hydrogen atom it was found [40] that $\alpha(0)\equiv\alpha_a(0)=4.50\,\text{a.u.}$ and $\omega_0\equiv\omega_{0a}=11.65\,\text{eV}$ (remind that $1\,\text{a.u.}$ of polarizability is equal to $1.482\times10^{-31}\,\text{m}^3$). For a hydrogen molecule it holds that [40] $\alpha(0)\equiv\alpha_m(0)=5.439\,\text{a.u.}$ and $\omega_0\equiv\omega_{0m}=14.09\,\text{eV}$.

In Fig. 1(a) we present the computational results for the van der Waals coefficient $C_{3,\text{H}}$ (in atomic units) for a hydrogen atom interacting with graphene as a function of separation. Note that one atomic unit for C_3 is equal to $4.032\times10^{-3}\,\text{eV}\,\text{nm}^3$. Computations were performed using Eqs. (6) and (8) with the hydrodynamic-model reflection coefficients (2) (the dashed line) and with the Dirac-model reflection coefficients (3) (the upper and lower solid lines obtained with the lower and upper bounds for graphene gap parameter Δ, respectively). As an upper bound, the value $0.1\,\text{eV}$ was chosen (see Sec. II). Keeping in mind that below some $\Delta_{\min}$ the values of C_3 are insensitive to further decrese of Δ (see below), the value of $10^{-15}\,\text{eV}$ was chosen as a lower bound. As is seen in Fig. 1(a), the values of $C_{3,\text{H}}$ computed using the hydrodynamic and Dirac models are significantly different and the ratio $C_{3,\text{H}}^{(h)}/C_{3,\text{H}}^{(D)}$ increases with the increase of separation distance. Thus, at the shortest separation $a=3\,\text{nm}$ it holds $C_{3,\text{H}}^{(h)}/C_{3,\text{H}}^{(D)}=1.065$. When separation varies to 5, 10, 20, 50, and $100\,\text{nm}$ this ratio increases to 1.19, 1.44, 1.85, 2.85, and 4.21, respectively (we have used the computational data related to the lower solid line with $\Delta=0.1\,\text{eV}$). At large separations of about $100\,\text{nm}$ both $C_{3,\text{H}}^{(h)}(a)$ and $C_{3,\text{H}}^{(D)}(a)$ decrease with separation as $1/a$ leading to $E_{\text{H}}^{(h,D)}(a)\sim1/a^4$. This is a typical behavior of the atom-plate interaction at relativistic separations [3–5] which holds also for other atomic systems considered below. In the nonretarded region $a<3\,\text{nm}$ the Casimir-Polder energy depends on separation as $a^{-7/2}$. This region is, however, outside the application region of our formalism based on the use of boundary conditions.

The relationship between the two solid lines in Fig. 1(a) demonstrates that the influence of the gap parameter on the value of $C_{3,\text{H}}$ is rather moderate. This is illustrated in more detail in Fig. 1(b) where $C_{3,\text{H}}$ is plotted as a function of $\log_{10}\Delta$. The solid lines labeled 1, 2, and 3 are computed at separations $a=5$, 50, and $100\,\text{nm}$, respectively. For the

line labeled 1 the relative difference between the maximum and minimum values of $C_{3,\mathrm{H}}$, $(C_{3,\mathrm{H}}^{\max}-C_{3,\mathrm{H}}^{\min})/C_{3,\mathrm{H}}^{\min}=6.6\%$. For the lines labeled 2 and 3 this relative difference is equal to 16.4% and 31.3%, respectively. For sufficiently small $\Delta_{\min}$ (different at each separation) $C_{3,\mathrm{H}}$ becomes constant and does not depend on further decrease of Δ. Thus, for lines labeled 1, 2, and 3 the van der Waals coefficient is constant for gap parameters satisfying the inequalities $\Delta\leq 0.01\,\mathrm{eV}$, $\Delta\leq 0.004\,\mathrm{eV}$, and $\Delta\leq 0.001\,\mathrm{eV}$, respectively.

The computational results for a hydrogen molecule differ from the respective results for a hydrogen atom quantitatively but not qualitatively. In Fig. 2 the van der Waals coefficient C_{3,H_2} is plotted as a function of separation [the dashed line is computed using the hydrodynamic model and the two solid lines using the Dirac model with the same gap parameters as in Fig. 1(a)]. Here, at the shortest separation $a=3\,\mathrm{nm}$ it holds $C_{3,\mathrm{H}_2}^{(h)}/C_{3,\mathrm{H}_2}^{(D)}=1.045$, i.e., the computational results are slightly closer than for a hydrogen atom. With the increase of separation to 5, 10, 20, 50, and 100 nm the ratio of the van der Waals coefficients computed using the two models increases to 1.18, 1.45, 1.89, 3.00, and 4.63, respectively, i.e., becomes larger than respective ratio for a hydrogen atom. As to the role of the gap parameter of graphene, its value only slightly influences the computational results. Figures 1(a) and 2 raise a question if it is possible to discriminate between the two models of graphene from experiments on quantum reflection. This question is considered in the next section.

IV. QUANTUM REFLECTION OF METASTABLE He^* AND Na ATOMS ON GRAPHENE

Experiments on quantum reflection [6–13] of cold atoms on different surfaces demonstrated that the reflection amplitude depends critically on the form of interaction potential. Because of this, using the experimental data for reflection amplitudes, it is possible to restore the form of potential within the limits of experimental error. If the two models of graphene (the hydrodynamic one and the Dirac one) lead to the values of interaction energy which differ dramatically, it might be possible to experimentally exclude some model or find it consistent with the data. To make reflection amplitudes more pronounced it is customary in experiments on quantum reflection to use atoms with large static electric polarizability. This allows to obtain more than one order of magnitude larger values of the van der Waals coefficient C_3 when compared to the values of the same coefficient for hydrogen atoms and

molecules plotted in Figs. 1(a,b) and 2.

We begin with an atom of metastable He* interacting with graphene by means of dispersion interaction. For He* atom it holds [41] $\alpha(0) \equiv \alpha_{\rm He^*}(0) = 315.63\,$a.u. and $\omega_0 \equiv \omega_{0,\rm He^*} = 1.18\,$eV. Computations were performed using Eqs. (6) and (8) with reflection coefficients, as defined in the hydrodynamic (2) or Dirac (3) models of graphene. The computational results for the van der Waals coefficients $C_{3,\rm He^*}$ as a function of separation are presented in Fig. 3 by the dashed line (the hydrodynamic model) and by the two solid lines (the Dirac model) obtained with two values of the gap parameter of graphene indicated in Sec. III. Similar to the case of hydrogen atom and molecule the ratio $C^{(h)}_{3,\rm He^*}/C^{(D)}_{3,\rm He^*}$ is larger than unity (it is equal to 1.33 at $a = 3\,$nm and increases with the increase of separation). At $a = 5$, 10, 20, 50, and 100 nm this ratio is equal to 1.47, 1.76, 2.23, 3.33, and 4.78. Thus, it is larger than for atoms and molecules of hydrogen at all separations. What is more important, the magnitudes of $C^{(D)}_{3,\rm He^*}$ computed with the Dirac model are by a factor of 18 (at $a = 3\,$nm) and by a factor of 46 (at $a = 100\,$nm) larger than respective values of $C^{(D)}_{3,\rm H}$ computed using the same model. In a similar way, $C^{(h)}_{3,\rm He^*}(3\,\rm nm) = 23C^{(h)}_{3,\rm H}(3\,\rm nm)$ and $C^{(h)}_{3,\rm He^*}(100\,\rm nm) = 52C^{(h)}_{3,\rm H}(100\,\rm nm)$. This makes experiments on quantum reflection of He* atoms on graphite feasible. Note that the role of thermal effects at separations considered is negligibly small. For example, we have computed the values of $C^{(D)}_{3,\rm He^*}$ at $a = 0.5\,\mu$m both at $T = 0$ and $T = 300\,$K using the zero-temperature and the thermal Lifshitz formulas. In the framework of the Dirac model the following respective values were obtained: $C^{(D)}_{3,\rm He^*} = 0.0183505\,$a.u. and $C^{(D)}_{3,\rm He^*} = 0.0183565\,$a.u. This means that at $a = 0.5\,\mu$m the relative difference between the results obtained using the zero-temperature and thermal Lifshitz formula is equal to only 0.033%.

It is interesting also to analyze the influence of a gap parameter of graphene on the value of $C_{3,\rm He^*}$ illustrated in Fig. 3 by the upper and lower solid lines computed with $\Delta = 10^{-15}\,$eV and with $\Delta = 0.1\,$eV, respectively. Thus, at $a = 5\,$nm it holds $(C^{\rm max}_{3,\rm He^*} - C^{\rm min}_{3,\rm He^*})/C^{\rm min}_{3,\rm He^*} = 3.7\%$. At separations $a = 50$ and 100 nm the same relative difference is equal to 28% and 46%, respectively. From this it follows that at large separations the impact of the value of a gap parameter Δ on $C^{(D)}_{3,\rm He^*}(a)$ is somewhat stronger than on $C^{(D)}_{3,\rm H}(a)$.

Another atom suitable in experiments on quantum reflection on graphene is Na. For Na atom it holds [42] $\alpha(0) \equiv \alpha_{\rm Na}(0) = 162.68\,$a.u. and $\omega_0 \equiv \omega_{0,\rm Na} = 1.55\,$eV. The computational results for the van der Waals coefficients $C^{(h)}_{3,\rm Na}$ (the dashed line) and $C^{(D)}_{3,\rm Na}$ (the two solid

lines for two values of the gap parameter indicated above) as a function of separation are presented in Fig. 4. At $a = 3\,\mathrm{nm}$ we obtain $C^{(h)}_{3,\mathrm{Na}}/C^{(D)}_{3,\mathrm{Na}} = 1.40$. With the increase of separation to $a = 5$, 10, 20, 50, and 100 nm this ratio increases to 1.55, 1.87, 2.39, 3.61, and 5.29, respectively. The magnitudes of $C^{(D)}_{3,\mathrm{Na}}$ are by a factor 11.6 (at $a = 3\,\mathrm{nm}$) and by a factor of 26 (at $a = 100\,\mathrm{nm}$) larger than the respective values of $C^{(D)}_{3,\mathrm{H}}$. In a similar way, $C^{(h)}_{3,\mathrm{Na}}(3\,\mathrm{nm}) = 15C^{(h)}_{3,\mathrm{H}}(3\,\mathrm{nm})$ and $C^{(h)}_{3,\mathrm{Na}}(100\,\mathrm{nm}) = 33C^{(h)}_{3,\mathrm{H}}(100\,\mathrm{nm})$. The exceeding of $C^{(h)}_{3,\mathrm{Na}}$ relative to $C^{(h)}_{3,\mathrm{H}}$ is not so large as for He^* atoms, but still sufficient for experimental purposes.

The upper and lower solid lines in Fig. 4 illustrate the influence of a gap parameter of graphene Δ on the value of $C_{3,\mathrm{Na}}$. Thus, at $a = 5\,\mathrm{nm}$ it holds $(C^{\max}_{3,\mathrm{Na}} - C^{\min}_{3,\mathrm{Na}}/C^{\min}_{3,\mathrm{Na}} = 3.2\%$. At separations $a = 50$ and 100 nm the relative difference between maximum and minimum values of $C_{3,\mathrm{Na}}$ is equal to 25.6% and 42%, respectively. These results are similar to the respective results for He^* atoms.

In almost all papers devoted to the experimental investigation of quantum reflection [6, 7, 11, 13] the comparison of the measurement data with theory is performed with the use of a phenomenological potential for the atom-wall interaction. This simplifies the calculation of theoretical reflection amplitudes to be compared with the experimental ones. The most often used phenomenological potential has the form [4–7, 11, 13]

$$E^{\mathrm{ph}}(a) = -\frac{C_4}{a^3(a+l)}, \tag{9}$$

where l is a characteristic parameter with the dimension of length that depends on the material of the plate. It is assumed that at short separations $a \ll l$ (typically at separations of a few nanometers where the retardation effects are negligibly small), $E^{\mathrm{ph}}(a)$ coincides with the van der Waals interaction energy between an atom and usual material plate [Eq. (5) with practically constant C_3], so that $C_4 = lC_3$. At large separations, where l is negligibly small in comparison with a, the phenomenological potential (9) coincides with the Casimir-Polder retarded interaction energy $-C_4/a^4$ obtained for ideal metal wall [3, 4]. The comparison of computational results obtained using Eq. (9) with measurement data for the reflection amplitudes allows one to determine the experimental values for the parameters l and C_4. Note that Eq. (9) does not agree with a nonretarded asymptotic limit for atom-graphene interaction (see Sec. III). As shown below, Eq. (9) provides a very good agreement with computations using the Lifshitz formula only at moderate separations. In Ref. [19] the accuracy of the phenomenological potential was investigated by the comparison with exact

results obtained using the Lifshitz theory. It was shown that the phenomenological potential leads to quantitatively correct results only in the limit of short separation distances below 100 nm. This conclusion was confirmed experimentally in Ref. [43] where deviations between the theoretical prediction using the phenomenological potential and the measurement data within the separation region from 160 to 220 nm were demonstrated. Below we use the phenomenological potential (9) only at separations below 100 nm and compare the obtained results with those using the Lifshitz theory. The separation regions where Eq. (9) leads to less than 1% error are specified.

Here, we perform the best fit of the phenomenological potential (9) to the energies $E^{(h)}(a)$ and $E^{(D)}(a)$ computed above for the interaction of He* and Na atoms with graphene described using the hydrodynamic and Dirac models, respectively. In doing so we first use the gap parameter of graphene $\Delta = 0.1\,\mathrm{eV}$. The results of the best fit of Eq. (9) to the dashed line in Fig. 3 (a He* atom interacting with graphene described by the hydrodynamic model) are the following:

$$C^{(h)}_{4,\mathrm{He}^*} = 85.11\,\mathrm{a.u.}, \qquad l^{(h)}_{\mathrm{He}^*} = 72.77\,\mathrm{nm}. \tag{10}$$

We note that 1 a.u. of C_4 is equal to $4.032\times10^{-3}\,\mathrm{eV\,nm}^4$. For the Dirac model, by making the best fit of Eq. (9) to the lower solid line in Fig. 3, we obtain

$$C^{(D)}_{4,\mathrm{He}^*} = 12.59\,\mathrm{a.u.}, \qquad l^{(D)}_{\mathrm{He}^*} = 11.18\,\mathrm{nm}. \tag{11}$$

It can be seen that the value of $E^{\mathrm{ph}}(a)$ from Eq. (9) with the parameters (10) deviate from the dashed line in Fig. 3 for less than 1% in the separation region from 10 to 60 nm. At the shortest and largest separations (3 and 100 nm, respectively) relative deviations achieve 10%. For the Dirac model, Eq. (9) with the parameters (11) deviates from the lower solid line in Fig. 3 for less than 1% at separations from 6 to 100 nm. The largest relative deviation of 5% holds at $a = 3\,\mathrm{nm}$. So large differences in the parameters of phenomenological potential, as predicted by the two models of graphene (by a factor of 6.8 for C_{4,He^*} and by a factor of 6.5 for l_{He^*}), make possible to decide between these models experimentally. The use of alternative values of the gap parameter leaves this conclusion unchanged. For example, repeating the same fit with $\Delta = 10^{-15}\,\mathrm{eV}$ (the upper solid line in Fig. 3) one arrives at $C^{(D)}_{4,\mathrm{He}^*} = 18.04\,\mathrm{a.u.}$ and $l^{(D)}_{\mathrm{He}^*} = 18.22\,\mathrm{nm}$. These are by factors 4.7 and 4.0 smaller than respective values (10) obtained using the hydrodynamic model of graphene.

Similar fit of Eq. (9) was performed to the lines of Fig. 4 representing the computational results for atoms of Na. This leads to

$$C_{4,\mathrm{Na}}^{(h)}=50.82\,\mathrm{a.u.},\qquad l_{\mathrm{Na}}^{(h)}=66.92\,\mathrm{nm} \tag{12}$$

for the hydrodynamic model and

$$C_{4,\mathrm{Na}}^{(D)}=7.11\,\mathrm{a.u.},\qquad l_{\mathrm{Na}}^{(D)}=9.77\,\mathrm{nm} \tag{13}$$

for the Dirac model of graphene. The energy (9) with parameters (12) deviates from the dashed line in Fig. 4 for less than 1% in the separation region from 10 to 60 nm. At separations of 3 and 100 nm the relative deviations achieve 11%. For the Dirac model, Eqs. (9) and (13) describe the lower solid line in Fig. 4 with less than 1% error in the region from 6 to 100 nm with maximum relative deviation of 5.7% at $a=3\,\mathrm{nm}$. Thus, for Na atoms the predictions of the two models of graphene for $C_{4,\mathrm{Na}}$ and l_{Na} differ by factors of 7.1 and 6.8, respectively. This makes possible an experimental choice between these two models. The above computations were performed with $\Delta=0.1\,\mathrm{eV}$. For the extremely small gap parameter $\Delta=10^{-15}\,\mathrm{eV}$ (the upper solid line in Fig. 4), one arrives at the values $C_{4,\mathrm{Na}}^{(D)}=9.74\,\mathrm{a.u.}$ and $l_{\mathrm{Na}}^{(D)}=15.45\,\mathrm{nm}$. These parameters of the phenomenological potential (9) are still less than the parameters obtained with the use of hydrodynamic model by factors of 5.2 and 4.3, respectively. This confirms that the experimental choice between the two models is possible with any value of the gap parameter.

V. CONCLUSIONS AND DISCUSSION

In the foregoing, we have investigated the van der Waals and Casimir-Polder interaction of different atoms with graphene on the basis of fundamental Lifshitz theory of atom-wall interaction. This was done by using the two approximate models of the electronic structure of graphene proposed in the literature, the hydrodynamic model and the Dirac model. The respective two sets of reflection coefficients for the electromagnetic oscillations on graphene were used in computations of the van der Waals coefficients describing dispersion interaction of hydrogen (H and H_2), and He^* and Na atoms with graphene as a function of separation. It was shown that the hydrodynamic and Dirac models of graphene lead to drastically different predictions for the strength of atom-graphene interaction. This conclusion was

obtained independently of the value of the gap parameter of graphene which was allowed to reduce from the experimental upper limit to almost zero.

Keeping in mind that both models of graphene are idealizations valid for different values of parameters, the new experiment was proposed capable to discriminate between the alternative theoretical predictions. For this purpose it was suggested to consider the quantum reflection of He^* and Na atoms on graphene. Due to large static electric polarizabilities, the van der Waals coefficients for the interaction of He^* and Na atoms with graphene were shown to be in several tens times greater than for H and H_2. This makes the observation of quantum reflection of He^* and Na atoms on graphene feasible. For the needs of proposed experiment, we have determined the parameters of phenomenological potential for He^* and Na atoms interacting with graphene described by both the hydrodynamic and Dirac models. It was shown that the parameters obtained using the hydrodynamic model are by a factor varying from 4.0 to 7.1 greater than the parameters obtained using the Dirac model. This demonstrates that the proposed experiment should be capable to discriminate between the predictions of the Dirac and hydrodynamic models of graphene.

In the future it is supposed to employ the Dirac model for the computation of dispersion interaction between graphene and material plates made of different materials and between various atoms and molecules and carbon nanotubes.

Acknowledgments

This work was supported by the Grant of the Russian Ministry of Education P–184. G.L.K. was also partially supported by CNPq (Brazil).

---

[1] J. Mahanty and B. W. Ninham, *Dispersion Forces* (Academic Press, London, 1976).

[2] V. A. Parsegian, *Van der Waals Forces: A Handbook for Biologists, Chemists, Engineers, and Physicists* (Cambridge University Press, Cambridge, 2005).

[3] H. B. G. Casimir and D. Polder, Phys. Rev. **73**, 360 (1948).

[4] M. Bordag, G. L. Klimchitskaya, U. Mohideen, and V. M. Mostepanenko, *Advances in the Casimir Effect* (Oxford University Press, Oxford, 2009).

[5] G. L. Klimchitskaya, U. Mohideen, and V. M. Mostepanenko, Rev. Mod. Phys. **81**, 1827 (2009).

[6] F. Shimizu, Phys. Rev. Lett. **86**, 987 (2001).

[7] H. Friedrich, G. Jacoby, and C. G. Meister, Phys. Rev. A **65**, 032902 (2002).

[8] H. Friedrich and J. Trost, Phys. Rep. **397**, 359 (2004).

[9] A. Jurisch and H. Friedrich, Phys. Lett. A **349**, 230 (2006).

[10] A. Yu. Voronin, P. Froelich, and B. Zygelman, Phys. Rev. A **72**, 062903 (2005).

[11] V. Druzhinina and M. DeKieviet, Phys. Rev. Lett. **91**, 193202 (2003).

[12] H. Oberst, D. Kouznetsov, K. Shimizu, J.-I. Fujita, and F. Shimizu, Phys. Rev. Lett. **94**, 013203 (2005).

[13] H. Oberst, Y. Tashiro, K. Shimizu, and F. Shimizu, Phys. Rev. A **71**, 052901 (2005).

[14] E. M. Lifshitz and L. P. Pitaevskii, *Statistical Physics*, Part. II (Pergamon Press, Oxford, 1980).

[15] J. F. Babb, G. L. Klimchitskaya, and V. M. Mostepanenko, Phys. Rev. A **70**, 042901 (2004).

[16] A. O. Caride, G. L. Klimchitskaya, V. M. Mostepanenko, and S. I. Zanette, Phys. Rev. A **71**, 042901 (2005).

[17] S. Y. Buhmann, L. Knöll, D.-G. Welsch, and H. T. Dung, Phys. Rev. A **70**, 052117 (2004).

[18] S. Y. Buhmann and D.-G. Welsch, Progr. Quant. Electronics **31**, 51 (2007).

[19] V. B. Bezerra, G. L. Klimchitskaya, V. M. Mostepanenko, and C. Romero, Phys. Rev. A **78**, 042901 (2008).

[20] H. Safari, D.-G. Welsch, S. Y. Buhmann, and S. Scheel, Phys. Rev. A **78**, 062901 (2008).

[21] G. Bimonte, G. L. Klimchitskaya, and V. M. Mostepanenko, Phys. Rev. A **79**, 042906 (2009).

[22] A. H. Castro Neto, F. Guinea, N. M. R. Peres, K. S. Novoselov, and A. K. Geim, Rev. Mod. Phys. **81**, 109 (2009).

[23] A. C. Dillon, K. M. Jones, T. A. Bekkedahl, C. H. Kiang, D. S. Bethune, and H. J. Heben, Nature (London) **386**, 377 (1997).

[24] A. Bogicevic, S. Ovesson, P. Hyldgaard, B. I. Lundqvist, H. Brune, and D. R. Jennison, Phys. Rev. Lett. **85**, 1910 (2000).

[25] E. Hult, P. Hyldgaard, J. Rossmeisl, and B. I. Lundqvist, Phys. Rev. B **64**, 195414 (2001).

[26] J. Jung, P. García-González, J. F. Dobson, and R. W. Godby, Phys. Rev. B **70**, 205107 (2004).

[27] J. F. Dobson, A. White, and A. Rubio, Phys. Rev. Lett. **96**, 073201 (2006).

[28] I. V. Bondarev and Ph. Lambin, Phys. Rev. B **70**, 035407 (2004).

[29] E. V. Blagov, G. L. Klimchitskaya, and V. M. Mostepanenko, Phys. Rev. B **71**, 235401 (2005).

[30] A. L. Fetter, Ann. Phys. (N.Y.) **81**, 367 (1973).

[31] G. Barton, J. Phys. A **37**, 1011 (2004).

[32] G. Barton, J. Phys. A **38**, 2997 (2005).

[33] M. Bordag, J. Phys. A **39**, 6173 (2006).

[34] M. Bordag, B. Geyer, G. L. Klimchitskaya, and V. M. Mostepanenko, Phys. Rev. B **74**, 205431 (2006).

[35] E. V. Blagov, G. L. Klimchitskaya, and V. M. Mostepanenko, Phys. Rev. B **75**, 235413 (2007).

[36] A. K. Geim and K. S. Novoselov, Nature Mater. **6**, 183 (2007).

[37] M. Bordag, I. V. Fialkovsky, D. M. Gitman, and D. V. Vaassilevich, Phys. Rev. B **80**, 245406 (2009).

[38] O. Kenneth and I. Klich, Phys. Rev. B **78**, 014103 (2008).

[39] G. Gómez-Santos, Phys. Rev. B **80**, 245424 (2009).

[40] A. Rauber, J. R. Klein, M. W. Cole, and L. W. Bruch, Surf. Sci. **123**, 173 (1982).

[41] R. Brühl, P. Fouquet, R. E. Grisenti, J. P. Toennies, G. C. Hegerfeldt, T. Köhler, M. Stoll, and C. Walter, *Europhys. Lett.* **59**, 357 (2002).

[42] A. Derevianko, W. R. Johnson, M. S. Safronova, and J. F. Babb, Phys. Rev. Lett. **82**, 3589 (1999).

[43] H. Bender, Ph. W. Courteille, C, Marzok, C. Zimmermann, and S. Slama, Phys. Rev. Lett. **104**, 083201 (2010).

Figures

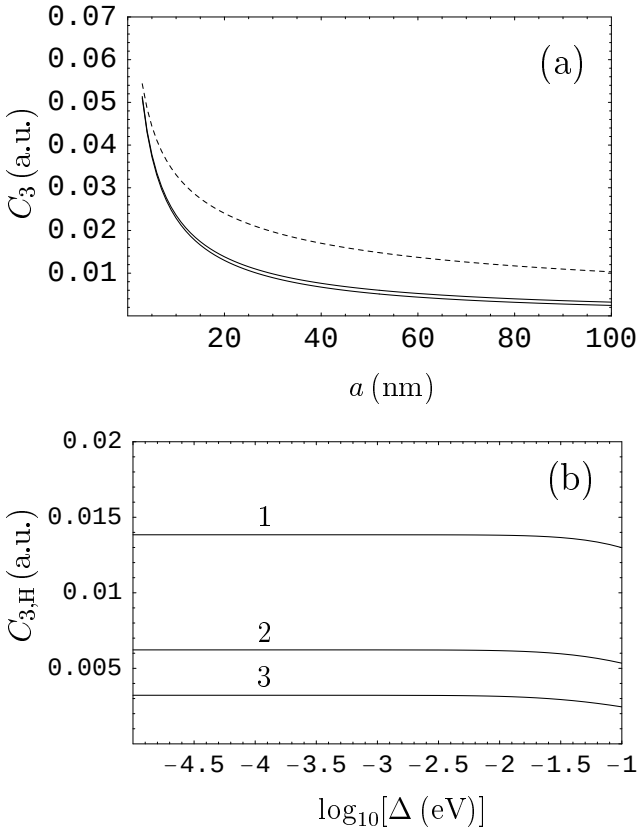

FIG. 1: The van der Waals coefficient for a H atom interacting with graphene as a function of (a) separation and (b) gap parameter. The dashed and the two solid lines are computed using the hydrodynamic model and the Dirac model with two different values of the gap parameter indicated in the text. The solid lines labeled 1, 2, and 3 are computed using the Dirac model at separations $a = 5$, 50, and 100 nm, respectively.

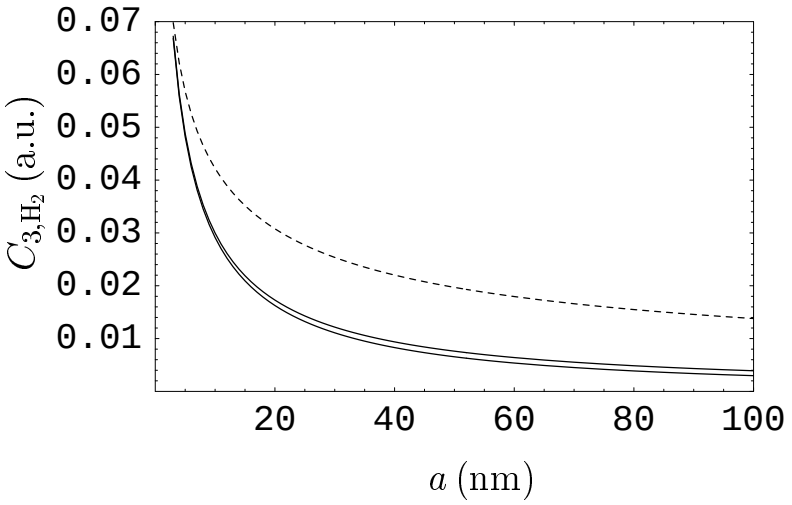

FIG. 2: The van der Waals coefficient for a H_2 molecule interacting with graphene as a function of separation. The dashed and the two solid lines are computed using the hydrodynamic model and the Dirac model with two different values of the gap parameter indicated in the text.

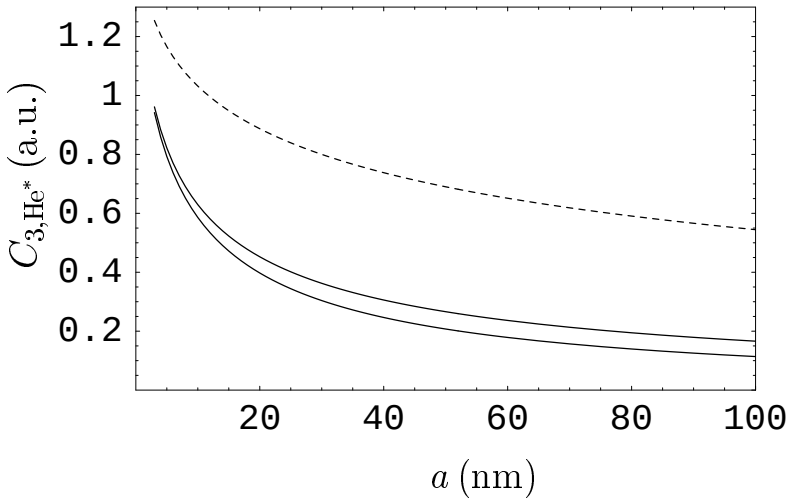

FIG. 3: The van der Waals coefficient for a He^* atom interacting with graphene as a function of separation. The dashed and the two solid lines are computed using the hydrodynamic model and the Dirac model with two different values of the gap parameter indicated in the text.

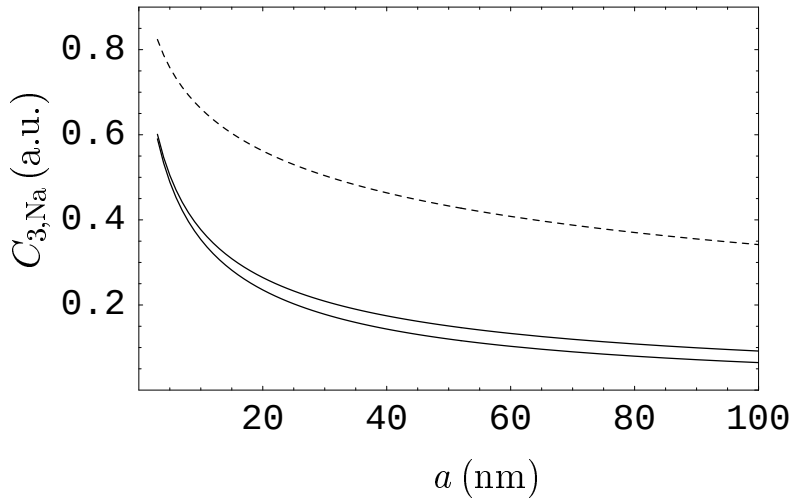

FIG. 4: The van der Waals coefficient for a Na atom interacting with graphene as a function of separation. The dashed and the two solid lines are computed using the hydrodynamic model and the Dirac model with two different values of the gap parameter indicated in the text.